Sculpting Fabrication of Nanocrater Catalysts and Exclusive Control of Wall Numbers and Diameters in Carbon Nanotubes

Kyung Min Choi, Saji Augustine, Young Min Kim, Ju Ho Lee, Jeong Yong Lee and Jeung Ku Kang*

[*] Prof. J. K. Kang, K. M. Choi, S. Augustine, J. H. Lee, Prof. J. Y. Lee

NanoCentury KAIST Institute, Graduate School of EEWS, Department of Materials Science & Engineering, KAIST, Daejeon, 305-701 (Korea).

E-mail: jeungku@kaist.ac.kr

Dr. Y. M. Kim

Division of Electron Microscopic Research, Korea Basic Science Institute, 52 Eoeun Dong, Yuseong -Gu, Deajeon, 305-806 (Korea).

Experimental Method

Synthesis of Nanocrater: Iron films of 15 nm thicknesses were deposited on silicon substrate using rf sputtering (100 Watt, 200 °C). Then, the substrate was moved to the microwave plasma enhanced chemical vapour deposition (MPECVD) chamber. The chamber was evacuated to a base vacuum pressure of about 0.1 Torr and the substrate was then subjected to N_2 plasma bombardment obtained for using a microwave power of 700 Watts at 800 °C. Subsequently, substrate was moved into a solution of CH_3CH_2OH: HNO_3:I_2 (5:1:1mg) for about 3.5 hours at room temperature.

Growth of Carbon Nanotubes: The CNTs were synthesized by MPECVD. The substrate was first evacuated followed by heating to 560 °C. A microwave having a frequency of 2.45 GHz was switched on to initiate a discharge in N_2 at a pressure of 18 Torr with a microwave power of 600 W. Subsequently, CH_4 at 15 sccm was introduced into the chamber and the microwave power was increased to 700 W. Under these conditions, aligned CNTs were found to grow on both the pristine as well as the nanocrater catalysts.

Detailed Analysis Methods

SEM, AFM, TEM, and EELS Analysis

The morphology, structure of nanocraters and as-grown CNT were analyzed *via* Field Emission SEM (Hitachi S-4800), Plane view TEM, cross-section TEM, high-resolution transmission electron microscopy (HRTEM) (FE-TEM F20, Phillips), and AFM (Digital Instruments, Veeco Metrology Group, Dimension TM 3100). In addition, the structure and chemical features of the cross-sectioned Fe nanocraters were analyzed using a high-voltage electron microscope (HVEM, JEM-ARM1300S, JEOL Inc.) operated at 1250 keV with a high-voltage gatan imaging filter (HV-GIF, Gatan Inc.). To identify the crystal structure of the nanocraters, a high-resolution transmission electron microscopy (HRTEM) was carried

out with the image calculation by multi-slice method. Spherical and chromatic aberration coefficients of the employed microscope are Cs = 2.6 and Cc = 4.1mm, respectively. The instrumental resolution of this microscope was 0.12 nm at Scherzer defocus (Δf = - 54 nm). The convergence semi-angle (α) of the incident electron beam was measured to be 0.5 mrad by the diffraction method, and the standard deviation (D) of the Gaussian distribution for the spread of focus is estimated to be 8 nm. Moreover, an electron energy loss spectroscopy (EELS) was employed to determine the chemical composition of crater structures. The near-edge fine structures of the characteristic oxygen K and iron L2, 3 edges were compared with the reference EELS spectrum of Fe_2O_3.

The plan view of the nanocraters by the Transmission Electron Microscope (TEM)

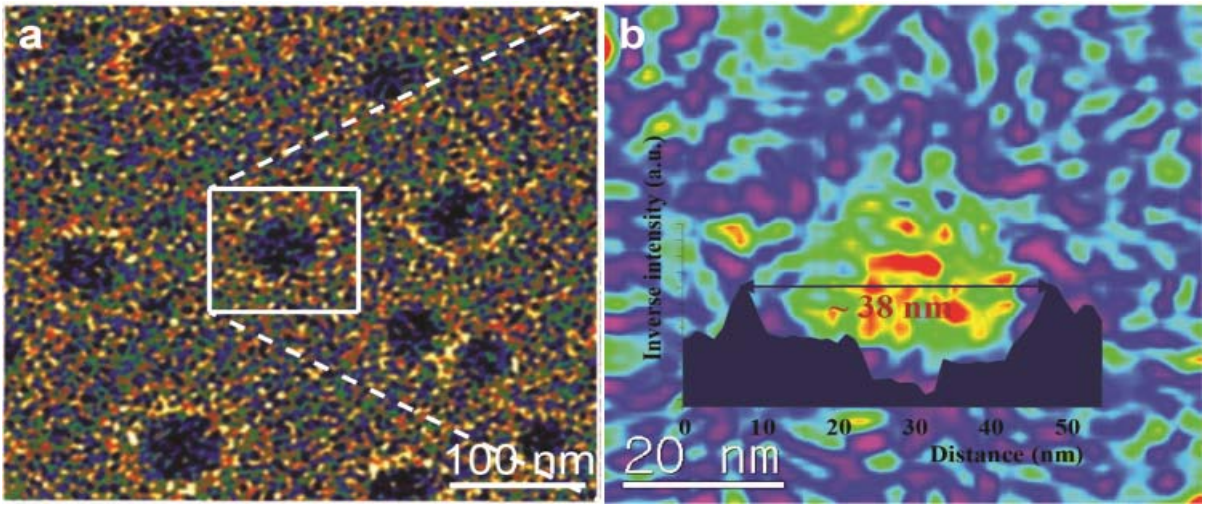

Figure S1. TEM Images of nanocraters. a) Plane view TEM image of Fe nanocraters. b) Inverse profile of horizontal electron intensities across the one of nanocrater in Figure S1a, which confirms its crater-like hollow particle structure of a nanocrater.

Detailed analysis for Electron Energy Loss Spectroscopy (EELS)

EELS measurement was performed to identify the elemental constituent of the nanocrater fabricated from Fe thin films. As shown in Fig. 2e, it is seen that the chemical composition of the nanocrater consists of Fe and O. The iron $L_{2,3}$ spectra for the Fe-O compounds in Fig. 2e shows a similar profile with two peaks labeled L_3 and L_2. Even though there must be the

difference of the intensity ratio (I_{L3}/I_{L2}) and the chemical shift of the two peaks depending on the oxidation state and coordination number for the iron ion in Fe-O compounds,[1] the region-of-interest of the sample in this experiment is too small to obtain a sufficient signal-to-noise ratio for the reliable interpretation of the Fe L spectrum. In addition, typical energy resolution (1.5 eV) and beam current stability in our spectrometer are not enough to resolve these differences. However, oxygen K edge in EELS spectra displays much distinct features with respect to the type of Fe-O compounds because the peaks in the spectra reflect a type of transition to the bound states.[2] The distinctive feature is whether the prepeak below ~530 eV of the dominant peak which remains rather similar for all phases of Fe-O system is discriminated or not. Many researchers have experimentally investigated oxygen K edges for various phases of Fe-O system with EELS techniques.[3] Among the Fe-O compounds (FeO, α-Fe_2O_3, γ-Fe_2O_3, and Fe_3O_4), the prepeak of oxygen K edge in FeO shows the least intensity. Even in conventional EELS spectrometer with low energy resolution, this intensity cannot be detected. The relative intensity of this prepeak gradually increases from FeO to Fe_2O_3. As a consequence, the local structure determined by EELS shows that chemical composition of the nanocrater structure is FeO because there is no evidence for the existence of the prepeak in O K edge. For a clear comparison, the reference spectrum for Fe_2O_3 is shown in Fig. 2e together with the experimental spectrum. The distinctive prepeak marked as the asterisk in the Fe_2O_3 spectrum is obviously different from the spectrum for FeO compound.

References

[1] J.Tafto, O. L., *Phys. Rev. Lett.* **1982**, *48*, 560.

[2] C. ColliexT. , Manoubi, C. Ortiz, *Phys. Rev. B* **1991**, *44*, 11402.

[3] L. A. Grunes, R. D. Leapman, C. N. Wilker, R. Hoffmann, A. B. Kunz, *Phys. Rev. B* **1982**, *25*, 7157.